Quantum dots based full-color display on MicroLED technology

CHIH-HAO LIN[1], CHUN-FU LEE[1], CHIEN-CHUNG LIN[2], CHEN-HSIEN CHU[2], CHIN-WEI SHER[3], ZHAO-JUN LIU[4], AND HAO-CHUNG KUO[1,*]

1Department of Photonics and Institute of Electro-Optical Engineering, National Chiao Tung University, Hsinchu 30010, Taiwan

2Institute of Photonic System, National Chiao Tung University, Tainan 711, Taiwan

3Fok Ying Tung Research Institute, Hong Kong University of Science and Technology, Hong Kong

4Department Of Electrical and Electronic Engineering, Southern University of Science and Technology, Shenzhen, China

*Corresponding author: hckuo@faculty.nctu.edu.tw

Abstract

In this paper, we would like to review our lab's result " a quantum-dot (QD)-based full-color emission red–green–blue (RGB) micro-light-emitting-diode (micro-LED) array ". By *using photoresist as the masking material for micro-LED arrays, also the photoresist mold can reduce optical cross-talk effect. The colloidal quantum dots (QDs) are used as photon conversion layer and the Aerosol Jet ® technology was applied for dispensing the QDs. A full-color array can be demonstrated and the isolation between pixels can be improved. The output light intensity can also be improved via the inclusion of a ultra-violet band distributed Bragg reflector (DBR).*

Author Keywords

micro LED, quantum dot, light emitting diode, micro display

1. Introduction

Recently, gallium-nitride-based (GaN) light-emitting diodes (LEDs) have attracted much attention due to their wide application in visible light communications, vehicle headlights, and backlight units (BLU) in liquid crystal displays (LCDs). The main benefits of GaN LEDs are low-power-consumption, low-cost, and highly luminous light source. Furthermore, now a day, many researchers put their efforts towards micro-LEDs having micrometer-scale (<100μm) size. The advantage of this technology over large-scale (scale of a few hundred micrometers) LEDs are their different properties such as high current density operation and as a result high optical power density [1]. By fabricating the micro-LEDs into an array, one can improve the brightness, and quality of BLU in an LCD display. However, it is a tedious task to grow three different light emitting units such as red–green–blue (RGB) on the same panel. by epitaxial or fabrication efforts. In order to solve this problem, an alternative emitting source of colloidal quantum dots (QDs) and exciting the QDs optically by the LEDs can be used. [2]. The QDs have various unique properties such as narrow emission linewidths, large-area color gamut and high quantum yield. In our previous research [3], a full-color emitting panel is fabricated by combining RGB QDs with micro-UV LEDs of 35 μm × 35 μm pixel size and in 128 × 128 arrays.

Generally, the main reason behind efficiency loss in case of LCD display is the backlight system. In which a large number of emitting photons are absorb by color filter. In case of to achieve expected optical power, it is required to operate display more than ten times of brightness. Hence, the present approach i.e. photo-luminescent (PL) QDs based micro-LEDs can replace the color filters and wider color gamut (1.52 times that of NTSC 1976). Color gamut was an evaluation metric, which was determined by the maximum colors in the display. Rec.2020., a new color triangle was devised to strictly define the color gamut standard. Our previous research demonstrated a QD micro display with over 80% of the color gamut of Rec. 2020 [4]. By accurately locating QDs on the micro-LED array by using the Aerosol Jet (AJ) technique realizes such a QD-LED display. However, even with the optimized AJ parameters in our previous test results, the cross-talk effect still occurred during the QD deposition because the overflow of QDs were accrued when the host solvent was evaporated. Meanwhile, the nanoparticles can be drawn towards to the edge and dropt, this called the "coffee ring" effect. In this research, the cross-talk effect is significantly reduced by using Aerosol Jet printing process with the photoresist (PR)-mold that to define the blocking wall and confine QDs field. Moreover, the addition of distributed Bragg reflector (DBR) can help UV light more effectively by re-absorption of QDs. Furthermore, the re-absorption of UV light also could prevent the human safety by UV exposure issues.

2. Micro-LED

For the application of display, the LED should be shrunk to micron level to function as a pixel, and it is named as micro-LED. As H. X. Jiang's group in Texas Technique University had reported the first fabrication of micro-LED chip with diameter of 12 μm in 2001 [5]. Micro-LED becomes a hot topic soon after the inception.

The field of application of LEDs will vary depending on the chip size. Generally speaking, the size of the traditional LED is larger than 200 μm, the mini-LED is between 100 to 200 μm, while the micro-LED is smaller than 100 μm. Therefore, the traditional LED chip is mainly used in general lighting and display backlight module, the mini-LED is applied to backlight applications such as HDR and flexible displays, while the micro-LED, a new display application, is suitable for applications such as wearable watches, mobile phones, automotive head-up displays, AR/VR, micro projectors, and high-end televisions. Additionally, micro-LED can be combined with a flexible substrate to realize the flexible characteristics like OLED (Table 1). Therefore, micro-LED displays have the potential to match or exceed the high contrast, low power consumption, high brightness of today's OLED displays without the lifetime issues that are associated with organic based display systems.

Table 1. Requirements for mini-LED and micro-LED in typical applications.

Application	Auto Display	TV	Digital Display
			
Panel Size (inch)	6 ~ 12	32 ~ 100	150 ~ 220
PPI	150 ~ 250	40 ~ 80	20 ~ 30
Chip volume (M)	4.1	24.9	24.9
Chip Size (μm)	50 ~ 100	50 ~ 80	80 ~ 100
Application	**AR**	**Watch**	**Mobile**
			
Panel Size (inch)	0.5 ~ 1	1 ~ 1.5	4 ~ 6
PPI	450 ~ 2000	200 ~ 300	300 ~ 800
Chip volume (M)	49.8	0.4	6.2
Chip Size (μm)	1 ~ 5	10 ~ 30	30 ~ 50

At present, micro-LED display technology mainly faces three challenges. First, the mass production and transfer of three-color micro-LED chips. Second, the fabrication of TFT substrates with micron-pixel pitch. Third, the full-color method for display applications. With the rapid development of technology, the first two problems are expected to be effectively solved. However, how to achieve the full-color display, has become a toughest problem for the subsequent development of Micro-LED. Next, we will discuss several main methods of the full-color display for micro-LEDs.

2.1. RGB micro-LED full-color display

The principle of RGB full-color display is mainly based on the law of three primary colors that can be combined to create all other colors in nature via a certain ratio setting. therefore, for RGB LEDs, different currents are applied to control the brightness of each LED to realize the combination of three primary colors and achieve the full-color display. It is the method that is usually employed in LED large screens. [6].

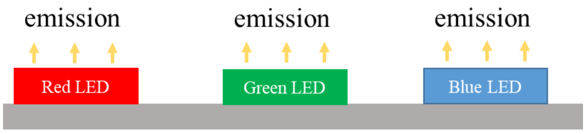

Figure 2. Mechanism of RGB micro-LED full-color display.

In the RGB full-color display method, each pixel contains a set of RGB micro-LEDs. Generally, the P and N electrodes of the three-color micro-LEDs are connected to the circuit substrate by means of bonding or flip-chip [7].

However, the RGB micro-LED based technology suffers a severe disadvantage in mass production. For example, in order to manufacture a 4K resolution display, nearly 25 million micro-LEDs are needed to be assembled and connected without a single error in an economical and efficient way, with placement accuracy of 1 μm or less. Obviously, it is very difficult to transfer or grow such a huge number of three different micro-LEDs on the same substrate.

2.2. Color conversion of full-color display

Excitation sources (UV micro-LED or blue micro-LED) with color-conversion materials can be used to achieve the full-color display. RGB color-conversion materials are needed to achieve RGB three primary colors if UV micro-LEDs are used, while only red and green color-conversion materials are required if blue micro-LEDs are used. Generally, color-conversion materials can be divided into the nano-phosphor and the quantum dots (QDs).

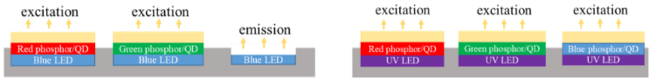

Figure 3. Mechanism of color conversion full-color display

2.3. Quantum dot

To realize full-color display, colloidal quantum dots (QDs) can be a great choice. The QDs are usually synthesized by chemical solution process [8] and possess unique properties such as high quantum yield, size-dependent emission wavelength, and narrow emission linewidth [9,10].

RGB QDs are in core-shell type structure with chemical ligands on the outer shells, and the average sizes of the QDs are 2.5 nm, 6.2 nm, and 9.3 nm for blue, green, and red QDs, respectively. The absorption and emission spectra for QDs are plotted in Figure 9(a), (c) and (e), while the images of the QDs in toluene under 365 nm UV light excitation are shown in Figure 9(b), (d) and (f). The wavelengths of emission spectra are 450 nm, 520 nm, and 630 nm for blue, green, and red QDs, respectively. Moreover, due to the narrow emission linewidths of RGB QDs, large-area color gamut can be readily achieved.

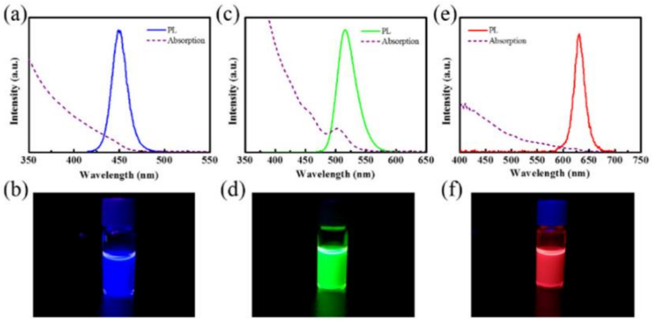

Figure 4. UV-visible absorption and PL emission spectra of QDs with the emission colors of (a) blue, (c) green and (e) red. (b) blue, (d) green and (f) red are the photos of QD solution under UV excitation.

3. RESULTS AND DISCUSSION

The micro-LED array with an emission wavelength of 395 nm, a single pixel size of 35 μm × 35 μm, and a pitch of 40 μm is fabricated. The total array number is 128 × 128 pixels in the chip area of 5 mm×5 mm. The UV micro-LED with RGB QDs has higher quantum yields than blue micro-LED. In order to reduce the optical cross-talk effect, a mold with open windows and blocking walls was fabricated with photoresist by simply lithography techniques. The Fig. 5 shows the region of the blocking wall that was formed by photoresist and UV lithography, and the height of the PR wall is 11.46 μm. The height of the blocking wall can be controlled by PR spinning processes, and we maintained it at thickness larger than 10μm. A silver coating is also applied to provide further isolation or the photon recycling.

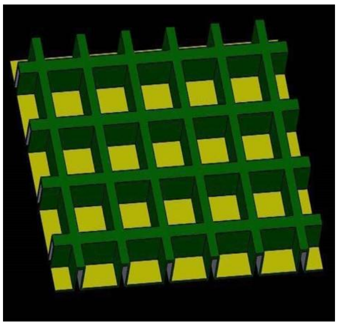

Figure 5. PR square windows with pixel size 35 μm × 35 μm, and the he laser scanner microscope image of the PR square wall.

The Fig. 6(a) shows the process flow for such device, the UV passive-matrix micro-LED array was fabricated on UV epi-wafers with a peak of 395 nm wavelength and a pitch size of 40 μm. The 128×128 pixels micro-LED pixels fabricated in the same column and sharing a common electrode of the n-type GaN. All of the stripes of the micro-LED array have been created individually by dry etching of GaN down to the sapphire substrate. On the dry etching process, SiO_2 was used as the hard mask. Finally, the p-electrode stripes were placed on top of the chips, and the n-electrode stripes were placed on the n-GaN layer, and all of the pixels are connected in the same row. The windows of the PR mold can be properly aligned to the micro-LED array, as shown in Figs. 6(b)–6(e), the AJ RGB QDs can be effectively deposited on the mold region, also prevent RGB QDs accrued overlay issue by the trench of PR wall. In order to fit the window size, the printing parameters are optimized. The adjustable parameters include the working distance between the nozzle and the substrate.

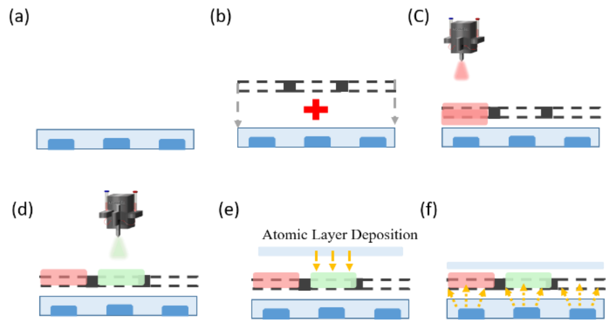

Figure 6. Process flow of the full-color micro display. (a) The structure of the micro-LED arrays. (b) Aligning the mold to the UV micro-LED array. (c)–(e) The process flow of the aerosol jet printing of RGB QDs on micro-LED array. (f) Coating Al_2O_3 ALD layer.

Table 2 summarizes the optimized parameters which includes working distance, carrier gas flow rate, the sheath gas flow rate, and the stage speed for the Aerosol Jet system®. During the dispense, the system will hold the working distance and the stage moving speed at constant to reduce the number of variables. Hence, only two parameters that we are changing here: the carrier gas flow rate and the sheath gas flow rate. In addition, the RGB different color of QDs have different particle sizes. Also the QDs are one of the components in the deposition, the different sizes of particles will affect the deposition rate. Hence, by adjusting the carrier flow rate and the sheath gas flow rate, we are able to find the best condition for the individual color of CQDs and obtained a good linewidth of 35μm in this study.

Table 2. Parameters of the AJ Printing Technique for Different QDs

QD Wavelength (nm)	Working Distance (mm)	Carrier Gas Flow Rate (sccm)	Sheath Gas Flow Rate (sccm)	Stage Speed (mm/s)
630	1	83	17	10
535	1	72	15	10
450	1	66	11	10

After we deposit the CQDs onto the molded glass substrate and align to the micro-LED array, the processes are finished. The Fig. 7 shows the different examples with and without molding walls can be shown. Both under regular OM and fluorescence OM can be seen, we find the intended channel is about 40.2 μm as mentioned in Fig. 7(a). Beside this, Fig. 7(b) show the overlap area of the red line is about 13.4 μm (the deviation between 53.4 and 40.2 μm). The blurred boundary between each color sub-pixel shows the possible leakage of photons into the other color and thus become the optical cross-talk. The cross talk can be defined as the photons astray into the neighboring pixels:

$$\text{Crosstalk}(\%) = \frac{\text{Leakage}}{\text{Intended channel}} \times 100\% \qquad \textbf{(1)}$$

where “Leakage” is the luminance of light that leaks from the unintended channel to the intended channel, which is defined as the overlap area. This method is largely based Wood’s research [11]. From the comparison of the light field distribution in Fig. 3, we could find that the molded case has almost all the colors contained within the pixel range, while the no-molding case has about 32.8% light distribution extended to next pixels.

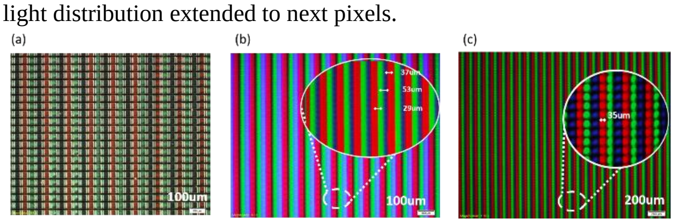

Figure 7. (a) Intended channel of the micro-LED layout with the pitch of 40.2 μm. (b) The previous result of cross-talk issue by without PR mold pixel array. (c) Observed the pixel array with PR mold by fluorescence microscopy.

In addition, this study resolves the coffee ring effect by the PR mold layer on micro-LED. The significant coffee ring effect that means QDs particle droplet and deposit along the surface tension to the edge when the host solvent was evaporated. Meanwhile, the nanoparticles can be drawn towards the boundary region, and this called the "coffee ring" effect as shown in Fig. 8(a) However, if we must to maintain the nanoparticles' feature without shrinkage issue, such a Nano-rippled surface exhibits hydrophobic characteristics and can be used to concentrate the droplets on the target area with a larger contact angle [12]. Hence, we demonstrate the walled pixel case (Fig. 4b), the wall formed a three-dimension container which can distribute the particle more evenly during the evaporation process such that the afterward distribution of CQDs are much uniform than before. This is more favorable than the regular no-molding case. [13–15].

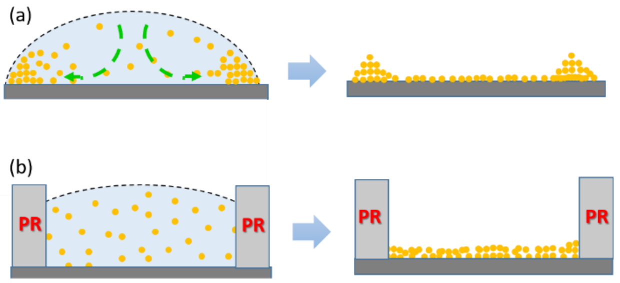

Figure 8. (a) The scheme of the coffee ring effect as show the outward flow issue caused by QDs evaporation loss. (b) The scheme of the PR mold design reduces the coffee ring effect.

Furthermore, the distributed Bragg reflector (DBR) technique will be an important applied on LED that to increase the UV light utilization by obtain a highly reflective interface to recycle the pumping photons. Regarding the DBR structure was composed of multiple pairs with different refractive index layer, we used the regular formula as follows [16, 17], where λ is the selected wavelength, the thickness d of the stacking dielectric materials depends on the refraction index and incidence angle θ, m is the number of stacked layers, and nsub, n1, and n2 represent the refractive indices of the substrate and the stacking dielectric layers, respectively. The DBR structure is prepared via alternative deposition of 17.5 pairs of HfO_2/SiO_2 multilayers on a quartz glass. The measurement peak of the DBR reflectance is 92.5% and the width of the stop band is 80 nm.

$$d = \lambda/(4n\cos\theta) \qquad \textbf{(2)}$$

$$R = |r|^2 = \left|\frac{\frac{n_{sub}}{n_1^2}(\frac{n_1}{n_1})^{2m}-1}{\frac{n_{sub}}{n_1^2}(\frac{n_1}{n_1})^{2m}+1}\right|^2 \qquad \textbf{(3)}$$

Then we assemble the DBR on QDs-deposited LED array, the measured of electroluminescence (EL) spectra shown in Fig. 9, the spectra reveal that the QDs enhanced the throughput about 23%, 32%, and 5% for red, green, and blue, respectively. The lower increase rate in blue band caused by the residual reflectance in the blue region of the DBR, which can cause the re-direct of the blue photons but lead to the extra loss. This can be further improved by optimized the DBR layer stack with a layer thickness of λ/(4n∗ cosθ).

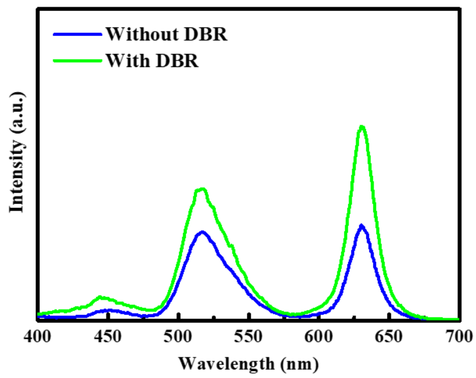

Figure 9. The measured EL spectra of RGB QDs on a UV micro-LED array, where the black and blue lines represent the devices with and without the DBR, respectively

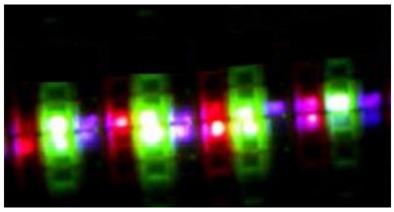

Figure 10. Light-up a row of the RGB pixel

Finally, we estimate the conversion efficiency of the RGB QDs by defined the optical conversion efficiency (OCE) to calculate the ratio of the energy transfer. To properly evaluate this number, an analysis on the emission spectra can reveal such information. From the previous study [18], we can use the following formula:

$$\frac{\text{Visible photons}}{\text{UV photons}} = \frac{\int \frac{\lambda}{hc}[I_{\text{emi}}^{\text{QD}}(\lambda) - I_{\text{emi}}^{\text{UV based}}(\lambda)]}{\int \frac{\lambda}{hc}[I_{\text{exc}}^{\text{UV based}}(\lambda) - I_{\text{exc}}^{\text{QD}}(\lambda)]} \qquad \textbf{(4)}$$

where $I_{emi}^{QD}(\lambda)$ and $I_{emi}^{UV\ based}$ are the integrated emission intensities in the visible band of the spectrum with and without QDs, and $I_{exc}^{QD}(\lambda)$ and $I_{exc}^{UV\ based}(\lambda)$ are the integrated intensities excited by UV light with and without QDs, respectively [19,20]. By calculation, the conversion efficiencies of the blue, green, and red CQDs layer are represent 2.25%, 10.8%, and 6.9%, respectively. The reason for the lower OCE values is related a protected issue during fabrication procedure, the efficiency of QDs would decrease by following reason, such influence come from moisture, oxidation, and heat. We will design a protected method that to optimize reliability in the future.

4. MATERIALS AND METHODS

A. Fabrication of the UV Micro-LED Array

The epitaxial structure of the UV micro-LED was grown by metal organic chemical-vapor deposition, which consists of an undoped GaN buffer layer on a sapphire substrate, followed by n-GaN, a multiple quantum well with a peak emission wavelength of 395 nm, p-GaN, and a current-spreading layer (CSL) for metal contact. The UV micro-LED array was fabricated by following process: mesa dry etching down to n-GaN via inductively coupled plasma (ICP), p-metal deposition on the CSL, n-metal deposition on the n-GaN layer, and then the trench opened by ICP etching down to the sapphire substrate that to make each micro-LED in individually, and sidewall passivation by plasma-enhanced chemical vapor deposition deposited SiO2.

B. AJ System

The aerosol system consisted of two major parts: an ultrasonic atomizer and a spraying chamber. First, the RGB QDs with concentrations of 5 mg∕mL in solvent were prepared in a tube that is inside the ultrasonic atomizer, and then the suspension was atomized by the ultrasonic vibration. The resulting AJ was consequently transferred to the nozzle by nitrogen gas flow. After the nitrogen gas input, the AJ was tightly focused at the end of nozzle to produce small drops, enabling narrow linewidth and high resolution.

5. CONCLUSION

In conclusion, we demonstrated a full-color micro display with a combination of a UV micro-LED array, Photoresist Mold, and RGB QDs by AJ technique. The CQDs were confined by the photoresist mold which can provide as light blocking wall and help the distribution of CQD more uniform. Furthermore, the optical cross-talk effect was also reduced with PR mold. A HfO2 ∕ SiO2 DBR stack can boost the efficient of UV light by recycling the pumping photons and enhanced intensity of QD emission as high as about 32% measured. The high-quality micro displays can be achieved by these techniques. We believe this technology can be helpful for next generation of micro-display platform.

6. Future Work

However, the best scale of linewidth is 35 µm in this research. Regarding this test result, this is still insufficient good enough to achieve our objective in Micro LED field. Hence, we participate with SIJ Technology on super inject printing project. Regarding the latest test result, the linewidth can well control around 25 µm with super fine nozzle as shown in Figure 11.

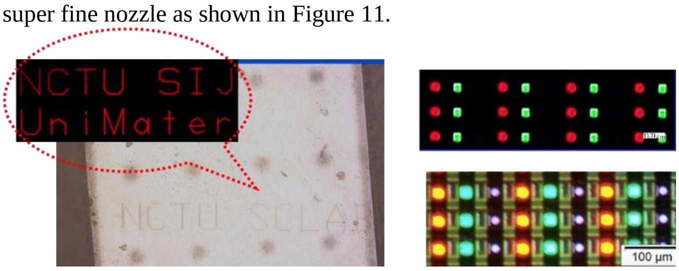

Figure 11. (a) the pattern of NCTU with 7.5µm linewidth. (b) observed RG QDs on Micro LED array. (c) observed the full color conversion by igniting Micro LED array. *(Source: SIJ Technology, Inc)*

Acknowledgment.
The authors would like to thank the Electronic and Optoelectronic System Research Laboratories of the Industrial Technology Research Institute and the Ministry of Science and Technology of Taiwan and SIJ Technology, Inc for their financial and technical support.

REFERENCES

[1] J. Herrnsdorf, J. J. McKendry, S. Zhang, E. Xie, R. Ferreira, D.Massoubre, A. M. Zuhdi, R. K. Henderson, I. Underwood, and S. Watson, “Active-matrix GaN micro light-emitting diode display with unprecedented brightness,” IEEE Trans. Electron Devices 62, 1918–1925 (2015).

[2] K. J. Chen, H. C. Chen, K. A. Tsai, C. C. Lin, H. H. Tsai, S. H. Chien, B. S. Cheng, Y. J. Hsu, M. H. Shih, and C. H. Tsai, “Resonant- enhanced full- color emission of quantum- dot- based display technology using a pulsed spray method,” Adv. Funct. Mater. 22, 5138–5143 (2012).

[3] H.-V. Han, H.-Y. Lin, C.-C. Lin, W.-C. Chong, J.-R. Li, K.-J. Chen, P.Yu, T.-M. Chen, H.-M. Chen, and K.-M. Lau, “Resonant-enhanced fullcolor emission of quantum-dot-based micro-LED display technology,” Opt. Express 23, 32504–32515 (2015).

[4] R. Zhu, Z. Luo, H. Chen, Y. Dong, and S.-T. Wu, “Realizing Rec. 2020 color gamut with quantum dot displays,” Opt. Express 23, 23680–23693 (2015).

[5] Jin, S.X.; Li, J.; Li, J.Z.; Lin, J.Y.; Jiang, H.X. GaN microdisk light emitting diodes. Applied Physics Letters 2000, 76, 631-633, 10.1063/1.125841.

[6] Geffroy, B.; Le Roy, P.; Prat, C. Organic light-emitting diode (OLED) technology: materials, devices and display technologies. Polymer International 2006, 55, 572-582, 10.1002/pi.1974.

[7] Peng, D.; Zhang, K.; Chao, S.D.; Mo, W. Full-Color Pixelated-Addressable Light Emitting Diode on Transparent Substrate (LEDoTS) Micro-Displays by CoB. Journal of Display Technology 2016, 12, 742-746.

[8] Mattoussi, H.; Mauro, J.M.; Goldman, E.R.; Anderson, G.P.; Sundar, V.C.; Mikulec, F.V.; Bawendi, M.G. Self-assembly of CdSe-ZnS quantum dot bioconjugates using an engineered recombinant protein. J. Am. Chem. Soc. 2000, 122, 12142-12150, 10.1021/ja002535y.

[9] Shirasaki, Y.; Supran, G.J.; Bawendi, M.G.; Bulovic, V. Emergence of colloidal quantum-dot light-emitting technologies. Nature Photon. 2013, 7, 13-23, 10.1038/nphoton.2012.328.

[10] Medintz, I.L.; Uyeda, H.T.; Goldman, E.R.; Mattoussi, H. Quantum dot bioconjugates for imaging, labelling and sensing. Nature Mater. 2005, 4, 435-446, 10.1038/nmat1390.

[11] A. J. Woods, “Crosstalk in stereoscopic displays: a review,” J. Electron. Imaging 21, 040902 (2012).

[12] Guoqiang Li, Jiawen Li, Chenchu Zhang, Yanlei Hu, Xiaohong Li, Jiaru Chu, Wenhao Huang, and Dong Wu, “Large-Area One-Step Assembly of Three-Dimensional Porous Metal Micro/Nanocages by Ethanol-Assisted Femtosecond Laser Irradiation for Enhanced Antireflection and Hydrophobicity,” ACS Appl. Mater. Interfaces 7, 383–390 (2015).

[13] R. D. Deegan, O. Bakajin, T. F. Dupont, G. Huber, S. R.

Nagel, and T. A. Witten, “Capillary flow as the cause of ring stains from dried liquid drops,” Nature 389, 827–829 (1997).
[14] C. Jiang, Z. Zhong, B. Liu, Z. He, J. Zou, L. Wang, J. Wang, J. Peng, and Y. Cao, “Coffee-ring-free quantum dot thin film using inkjet printing from a mixed-solvent system on modified ZnO transport layer for light-emitting devices,” ACS Appl. Mater. Interfaces 8, 26162–26168 (2016).
[15] S.-W. Wang, H.-Y. Lin, C.-C. Lin, T. S. Kao, K.-J. Chen, H.-V. Han, J.-R. Li, P.-T. Lee, H.-M. Chen, and M.-H. Hong, “Pulsed-laser micropatterned quantum-dot array for white light source,” Sci. Rep. 6, 23563 (2016).
[16] I. García, J. Geisz, M. Steiner, J. Olson, D. Friedman, and S. Kurtz, “Design of semiconductor-based back reflectors for high Voc monolithic multijunction solar cells,” in 38th IEEE Photovoltaic Specialists Conference (PVSC) (IEEE, 2012), p. 002042.
[17] H. K. H. Choy, “Design and fabrication of distributed Bragg reflectors for vertical-cavity surface-emitting lasers,” in IEEE International Conference on Semiconductor Electronics (Citeseer, 1998).
[18] K. Suzuki, A. Kobayashi, S. Kaneko, K. Takehira, T. Yoshihara, H. Ishida, Y. Shiina, S. Oishi, and S. Tobita, “Reevaluation of absolute luminescence quantum yields of standard solutions using a spectrometer with an integrating sphere and a back-thinned CCD detector,” Phys. Chem. Chem. Phys. 11, 9850–9860 (2009).
[19] S. C. Hsu, Y. H. Chen, Z. Y. Tu, H. V. Han, S. L. Lin, T. M. Chen, H. C. Kuo, and C. C. Lin, “Highly stable and efficient hybrid quantum dot light-emitting diodes,” IEEE Photon. J. 7, 1–7 (2015).
[20] S.-C. Hsu, L.-A. Ke, H.-C. Lin, T.-M. Chen, H.-Y. Lin, Y.-Z. Chen, Y.-L. Chueh, H.-C. Kuo, C.-C. Lin, "Fabrication of a Highly Stable White Light-Emitting Diode with Multiple-Layer Colloidal Quantum Dots", IEEE Journal of Selected Topics in Quantum Electronics, Vol. 23, No.5, p.1-9, 2017.